

Load Balancing in Two-Tier Cellular Networks with Open and Hybrid Access Femtocells

Dongmyoung Kim, Taejun Park, Hyoil Kim, and Sunghyun Choi

Abstract—Femtocell base station (BS) is a low-power, low-price BS based on cellular communication technology. It is expected to become a cost-effective solution for improving the communication performance of indoor users, whose traffic demands are large in general. There are mainly three access strategies for femtocell, i.e., closed access, open access and hybrid access strategies. While it has been generally known that open/hybrid access femtocells contribute more to enhancing the system-wide performance than closed access femtocells, the operating parameters of both macro and femtocells should be carefully chosen according to the mobile operator's policy, consumer's requirements, and so on. We propose long-term parameter optimization schemes, which maximize the average throughput of macrocell users while guaranteeing some degree of benefits to femtocell owners. To achieve this goal, we jointly optimize the ratio of dedicated resources for femtocells as well as the femtocell service area in open access femtocell networks through the numerical analysis. It is proved that the optimal parameter selection of open access femtocell is a convex optimization problem in typical environments. Then, we extend our algorithm to hybrid access femtocells where some intra-femtocell resources are dedicated only for femtocell owners while remaining resources are shared with foreign macrocell users. Our evaluation results show that the proposed parameter optimization schemes significantly enhance the performance of macrocell users thanks to the large offloading gain. The benefits provided to femtocell users are also adaptively maintained according to the femtocell users' requirements. The results in this paper provide insights about the situations where femtocell deployment on dedicated channels is preferred to the co-channel deployment.

Keywords—Femtocell, two-tier cellular networks, load balancing, coverage control.

I. INTRODUCTION

A FEMTOCELL base station abbreviated as femto BS or fBS is a small BS with low transmission power and low cost. Femtocells can be installed by the end users to enhance the cellular networking performance at home, of which traffic is transported via an Internet backhaul such as Digital Subscriber Line (DSL) or cable modem. Two-tier cellular networks, consisting of a conventional macrocell network and underlaying short-range femtocells, have received considerable attention from industry and academia as an efficient solution to deal with the exploding demand for wireless data communication. The femtocell technology has an advantage over other competing indoor wireless communication technologies, thanks to its high capacity and backward compatibility with existing cellular technologies. The history, current status of market and technology, research issues, and future expectation of femtocell technology are well summarized in [1].

There are mainly three strategies for a femtocell access, namely, closed access, open access, and hybrid access strate-

gies. A femtocell in a closed access mode can only be accessed by authorized femtocell users. On the other hand, if the owner of a femtocell installs it with the open access mode, any macrocell user might access the femtocell. Some previous researches [2]–[4] have shown that the deployment of open access femtocells can improve the system-wide performance by transferring some of the traffic loads in congested macrocells to the femtocells. Hybrid access mode is a compromise between closed and open access, where an fBS allows arbitrary nearby users to access it like open access mode but the subscribed femtocell owners can be prioritized over unsubscribed users. The prioritization can be implemented by using various vendor-specific mechanisms. In 3GPP Release 8 specification [5], only closed and open access modes are supported for femtocells while the hybrid access mode has been added in 3GPP Release 9 specification [6]. Therefore, considering both the open and hybrid access strategies is important.

In this paper, we numerically analyze and optimize the performance of both open and hybrid access femtocell networks. We propose the load balancing schemes which properly balance the traffic loads in macrocells and femtocells. Our load balancing schemes aim at maximizing the system-wide performance, i.e., the average throughput of the users communicating with the macrocells, in two-tier cellular networks with open or hybrid access femtocells, while guaranteeing some benefits of the femtocell owners such that femtocell users can always achieve larger throughput than macrocell users. Such an approach not only improves the macrocell user's performance via traffic offloading from macrocell to femtocell, but also promotes the deployment of femtocells via the guaranteed benefit to the femtocell owners.

In our proposed framework, we strike a balance between a macrocell and femtocells by controlling the service area of femtocells because the amount of traffic loads is dominated by the number of associated users. In order to maximize the offloading efficiency, orthogonal deployment — in which the whole wireless resources are divided into two parts, one dedicated to femtocells and the other reserved for a macrocell — is considered, and we jointly optimize the amount of resources dedicated to the femtocells and the service area of femtocells. The optimization problem is first studied for the open access case, and then extended to the hybrid access femtocell networks, where a variable portion of intra-femtocell resources is exclusively used by femtocell owners while remaining resources are shared with macrocell users associated with the femtocell.

The contributions of this paper are summarized as follows:

- 1) We numerically analyze the performance of macrocell

and femtocell users in two-tier cellular networks where open and hybrid access fBSs are deployed in an unplanned manner.

- 2) Multiple essential parameters in the open and hybrid access femtocell networks are jointly optimized to enhance the performance of both the macrocell and femtocell users.
- 3) Our results show that the orthogonal spectrum dedication for open and hybrid access femtocell can be more beneficial than co-channel deployment in some aspects. The conditions that femtocell deployment on dedicated channel can be preferred are also discussed.
- 4) It is proved that the joint optimization of the amount of dedicated resources and the service area of femtocells is a convex optimization problem in typical environments.

The rest of the paper is organized as follows. Section II presents the related work. In Section III, we introduce the system model and our load balancing problem formulation in the open and hybrid access femtocell based two-tier cellular networks. We analyze the average throughput of each type of users in Section IV to complete the problem formulation. In Section V, we obtain the optimal parameters of open access femtocell networks and some theorems for optimal parameter selection are discussed. By extending the optimization framework of open access femtocell networks, system parameters of hybrid access femtocell are also optimized in Section VI. In Section VII, our proposed schemes are evaluated based on both numerical analysis and computer simulations. Finally, we conclude the paper in Section VIII.

II. RELATED WORK

Many resource allocation schemes have been proposed for the two-tier cellular networks, but most of the proposed schemes are heuristic or locally optimized schemes [7]–[16]. On the other hand, some previous work conducts optimization based on full channel information [17]–[19] or game theoretic model [20]–[23]. Therefore, the previous researches are different from our work which optimizes the system-wide performance based on the long-term system information of the two-tier cellular networks where fBSs are deployed in an unplanned manner. Our long-term parameter optimization framework is not incompatible with but complementary to the short-term resource allocation schemes in the sense that the long-term optimization framework can provide good guidelines for the parameter configuration considering the system-wide average performance.

Recent papers [12], [24] are the most relevant previous work in the literature. Coverage control schemes have been proposed in [12], [25]. The authors in [12] proposes an adaptive transmit power control scheme to control the shape and the size of femtocell coverage. In closed access femtocell networks, which is the system model of the above mentioned papers, the objective of coverage control is minimizing the interference leakage from fBSs to the outdoor macrocell region while the expected service area for the subscribed users is guaranteed. Service area adaptation in this paper is different because the strong signal received from a femtocell is considered a good

serving signal in open and hybrid access femtocell networks, which allow the macrocell users to access them.

In [24], the authors propose a bandwidth division scheme in the two-tier cellular networks composed of the closed access femtocells. The objective and constraints of [24] are different from our work since ours utilizes the traffic offloading gain in the open and hybrid access femtocell networks. Furthermore, we optimize some other control parameters, such as target service area of a femtocell and intra-femtocell resource dedication ratio for a femtocell owner, together with the bandwidth division ratio to enhance the system performance.

III. SYSTEM MODEL AND OUR FRAMEWORK

A. System Model

We assume a single circular macrocell region with the radius of D_m and the area of $A_m = \pi D_m^2$, where a macrocell BS (mBS) is located at the center of the circular region. Multiple fBSs are randomly distributed within the macrocell region according to a homogeneous Spatial Poisson Point Process (SPPP) [26] with intensity λ_f . In an SPPP, the number of points in a given region follows Poisson random variable with the mean of λA , where λ and A are the intensity of the points and the area of the given region, respectively. We assume that each fBS is owned by a femtocell mobile station (fMS), and the fBS is located at the center of the indoor circular home region with the radius of D_h . The fMS of each fBS is randomly located within the circular home region, and the indoor home area and outdoor area are partitioned with a wall.

It is possible that the fBSs following SPPP are located closer than $2D_h$ to each other thus resulting in overlapping home areas. Although this should not happen in practice, we argue that the proposed SPPP model still well captures the reality because it is highly unlikely to have such overlapping fBSs with the practical range of λ_f and D_h . Suppose we denote by $P_{overlap}$ the probability that two or more fBSs overlap with each other. Since $P_{overlap}$ is identical to the probability that two or more fBSs exist in the area of $\pi(2D_h)^2$, we have

$$\begin{aligned} P_{overlap} &= 1 - e^{-\lambda_f \cdot 4\pi D_h^2} - \lambda_f \cdot 4\pi D_h^2 \cdot e^{-\lambda_f \cdot 4\pi D_h^2} \\ &= \begin{cases} 0.079, & \text{in US,} \\ 0.081, & \text{in Korea,} \end{cases} \end{aligned}$$

where the values of λ_f and D_h are obtained from [27], [28]. Hence, we henceforth assume that there exists only one fBS per home, i.e., the distance between any two fBSs is larger than $2D_h$. In Section VII, it will be verified that such an approach approximates typical environments with a reasonably small analytical error (less than 1 %) as shown in Fig. 6(a). Note that in our simulation, we generate fBSs according to SPPP and drop a new fBS located closer than $2D_h$ to any of the previously-generated fBSs.

Similarly to fBSs, macrocell users are randomly distributed according to an SPPP with intensity λ_u in the whole macrocell area. Because some macrocell users can associate with a nearby femtocell in the open and hybrid access femtocell networks, the macrocell users are categorized into two types,

TABLE I. TRANSMISSION RATE SET

Rate index, l	Spectral efficiency, b_l (bps/Hz)	SINR region (dB)
1	0.4922	$[-4, 0)$
2	1.3889	$[0, 4)$
3	2.8962	$[4, 8)$
4	4.7364	$[8, 12)$
5	6.6885	$[12, 16)$
6	8.6711	$[16, \infty)$

i.e., macrocell mobile station (mMS) and open access mobile station (oMS). We refer to the macrocell user who associates with mBS as mMS, while the macrocell user who associates with an fBS thanks to the open or hybrid access policy is referred to as oMS.

The downlink channel gain between a BS and an MS is characterized by a pathloss and fading. When the distance between a transmitter and a receiver is d , the channel gain of the link is modeled by $\Psi(Zd)^{-\alpha}$, where α is the pathloss exponent and Z represents a fixed loss which is dependent on the type of the link. Different Z and α values, i.e., Z_1 to Z_5 and α_1 to α_5 , are defined for different types of links as shown in Table III. $\Psi \sim \exp(1)$ is a Rayleigh fast fading component which has a unit average power.

We consider multiple discrete transmission rates, where the rate is adaptively determined according to the Signal to Interference plus Noise Ratio (SINR) value at the receiver. Rate index $l \in [1, L]$ corresponds to the case when the SINR lies in $[\Gamma_l, \Gamma_{l+1})$, where $\Gamma_{L+1} = \infty$. and the spectral efficiency of rate index l is modeled as the following based on the variable rate M-QAM transmissions:

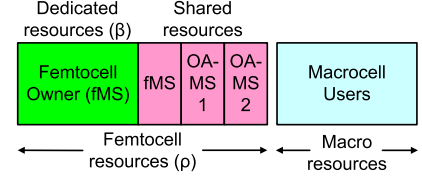
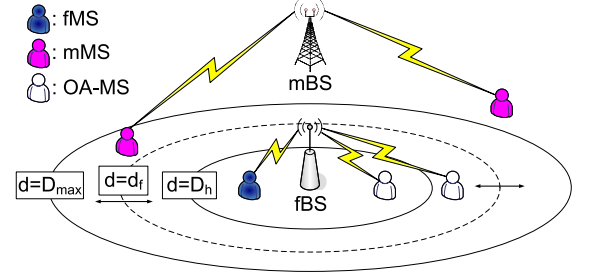
$$b_l = \log_2 \left(1 + \frac{\Gamma_l}{G} \right), \quad (1)$$

where G denotes Shannon Gap introduced in [29]. The specific rate set used in the simulations are summarized in Table I. Furthermore, Table II provides the definitions and default values of all notations frequently used in this paper.

In this paper, we consider a fully loaded network environment where the BSs always have packets to transmit. Furthermore, we assume that the scheduler in the mBS or the open access fBS allocates the resource blocks in a round-robin manner so that the whole wireless resources in the cell are equally distributed to the associated users in a long-term. The basic level of fairness, i.e., intra-cell resource fairness, is guaranteed from this assumption. In the hybrid access fBS, the scheduler reserves some amount of resources for the fMS while the remaining resources are allocated using a round-robin manner. We assume that the transmission power spectral densities, i.e., power per Hz, of the mBS and fBSs are fixed as P_m and P_f , respectively, and the noise power density is given by P_N .

B. Our Framework

In this section, we introduce our load balancing framework for open and hybrid access femtocell networks. As shown in Fig. 1, our schemes divide the whole available resources into two orthogonal sub-parts, and the two parts are dedicated to

Fig. 1. Resource dedication in hybrid access femtocells (ρ and β).Fig. 2. Femtocell service radius (d_f) and user associations.

the macrocell and femtocells, respectively. We refer to the ratio of resources dedicated to the femtocells among the whole available resources as $\rho \in [0, 1]$, and we optimize ρ to properly balance the traffic loads in the macro and femtocells. We assume that the wireless resources can be divided either in time domain or frequency domain or both.

Our framework allocates the separate resources to the femtocells because the resource separation not only limits the side effect to the existing macrocell users due to the femtocell deployment but also maximizes the offloading capability in the two-tier cellular networks by increasing the maximum cell coverage. Though it has been generally said that open access femtocell networks prefer the co-channel deployment option, the results of this paper show that algorithms based on separate bandwidth can be more beneficial in some aspects thanks to the enhanced offloading gain and the increased flexibility to control the performance of fMSs, mMSs, and oMSs. Appendix C summarizes the benefits and preferred conditions of orthogonal deployment.

A hybrid access fBS allows the macrocell users to access like open access fBS, but the intra-cell resource scheduler gives priority to the fMS. It is different from the intra-cell resource allocation policy of the open access femtocell where the resources are equally allocated to all the users without distinguishing the fMS from the other macrocell users. As shown in Fig. 1, we assume that β fraction of intra-femtocell resources are dedicated to the fMS, and the remaining resources are equally shared by the fMS and oMSs. Open access femtocell is a special case of hybrid access femtocell where $\beta = 0$.

Our load balancing scheme in the open and hybrid access femtocell networks jointly optimizes the average service area of a femtocell as well as the amount of bandwidth dedicated to femtocells and the amount of intra-femtocell resource dedicated to an fMS. We optimize the service coverage of a femtocell because the cell selection based on the strongest

TABLE II. DEFINITION OF PARAMETERS AND DEFAULT VALUES

Symbol	Description	Default value
D_m, A_m	Radius and area of a macrocell region	800 m, πD_m^2
D_h, A_h	Radius and area of a home region	20 m, πD_h^2
f_c	Carrier frequency	2000 MHz
W	System bandwidth	5 MHz
P_N	Noise power density	-174 dBm/Hz
P_m	Macrocell transmit power density	46/W dBm/Hz
P_f	Femtocell transmit power density	23/W dBm/Hz
WL	Wall penetration loss	10 dB
Ψ	Rayleigh fading component	N/A
α, Z^α	Pathloss exponent and fixed loss value	See Table III
b_l, Γ_l	Spectral efficiency and SINR threshold for rate index l	See Table I
N_f, λ_f	Average number and intensity of fBSs in a macrocell area	30, $30/A_m$
N_u, λ_u	Average number and intensity of macrocell users (mMSs + oMSs)	200, $200/A_m$
ρ	Ratio of femtocell resources to the whole bandwidth, $\rho \in [0, 1]$	N/A
d_f, D_{\max}	Service radius of a femtocell region and maximum value of d_f , respectively	N/A
x	Average service area of a femtocell region, $x \in [X_{\min}, X_{\max}]$	N/A
θ	Resource usage probability in OA/HA-Thin, $\theta \in [0, 1]$	N/A
β	Ratio of resources reserved for an fMS to the whole resources of a hybrid access fBS, $\beta \in [0, 1]$	N/A
$\bar{T}_f, \bar{T}_m, \bar{T}_o$	Average throughput of fMS, mMS, and oMS	N/A
$M (K)$	Required ratio between average throughput of fMS (oMS) and mMS	10, 1
O_{\max}	Maximum average outage rate allowed for an oMS	0.15

RSS value is not efficient to promote the load balancing. Fig. 2 describes the system model for the service coverage optimization. We refer to the service radius of a femtocell as d_f , and the femtocell and macrocell users who are located closer than d_f associate with the femtocell rather than the macrocell. Each fBS is required to fully cover the indoor home area, i.e., $d_f \geq D_h$. The maximum service radius, i.e., D_{\max} , is constrained by the physical limitation to support wireless communications. In our work, D_{\max} is defined by the maximum distance where the average outage probability of an oMS is less than or equal to O_{\max} while the lowest transmission rate is used. The service radius is chosen in the range of $d_f \in [D_h, D_{\max}]$ to properly balance the traffic loads in macro and femtocells.

The service coverage adaptation is implemented by using a simple MS initiated Cell Selection (MSCS) scheme. In MSCS, the RSS threshold for femtocell association, which is referred to as P_{cs} , is determined, and an MS measures the average RSS values of transmitted signals from the neighboring mBSs and fBSs. If the MS finds some fBSs providing the average RSS larger than P_{cs} , the MS associates with the best fBS among them regardless of the RSS values from the mBSs. Therefore, the target femtocell radius d_f is directly related to P_{cs} by

$$P_{cs} = P_f (Z d_f)^{-\alpha}, \quad (2)$$

where P_f is the fixed transmission power density of the fBS. We optimize d_f instead of P_{cs} in this paper to simplify the presentation.

Then, we formulate our parameter optimization problem for load balancing in hybrid access femtocell networks. The same framework can be applied for the open access femtocell networks by setting $\beta = 0$. Deployment of open and hybrid access femtocells has an advantage that it can improve the performance of the macrocell users as well as the femtocell owners by transferring the traffic load in the congested macrocells to the femtocells. Though the open access is allowed, the fMSs expect a differentiated experience when they use

their femtocells at home. Guaranteeing the benefits of fMSs is very important to motivate the consumers to buy and install the femtocells. Therefore, we aim at maximizing the average performance of mMSs by controlling ρ , d_f , and β (hybrid access only), while guaranteeing the relative benefits of femtocell owners. Specifically, it is assumed that fMSs expect that their average femtocell throughput should be at least M times larger than the average throughput of mMSs though they allow the open access.

Denoting the average throughput of an fMS, mMS, and oMS by $\bar{T}_f(\rho, d_f, \beta)$, $\bar{T}_m(\rho, d_f, \beta)$, and $\bar{T}_o(\rho, d_f, \beta)$, respectively, our optimization problem is formulated as:

$$\max_{\rho, d_f, \beta} \bar{T}_m(\rho, d_f, \beta) \quad (3)$$

s.t.

$$\bar{T}_f(\rho, d_f, \beta) \geq M \bar{T}_m(\rho, d_f, \beta), \quad (4)$$

$$\bar{T}_o(\rho, d_f, \beta) \geq K \bar{T}_m(\rho, d_f, \beta), \quad (5)$$

$$D_h \leq d_f \leq D_{\max}, \quad (6)$$

$$0 \leq \rho \leq 1, \quad (7)$$

$$0 \leq \beta \leq 1. \quad (8)$$

The macrocell users might not want to associate with fBSs if the performance is degraded by the open access with fBSs. Therefore, the constraint (5) is additionally introduced to guarantee the minimum performance of oMSs. Because oMSs are not the subscribed users, K is configured as a value smaller than M , and we basically assume that $K = 1$.

Our optimization framework is a long-term parameter optimization based on the average system-wide performance metric. Though a short-term local resource allocation scheme might improve the performance of the local system efficiently, our long-term optimization is very meaningful in the following aspects.

First, the parameter optimization involving both the macrocells and femtocells is generally performed at a long-term interval due to the system architecture of the two-tier cellular

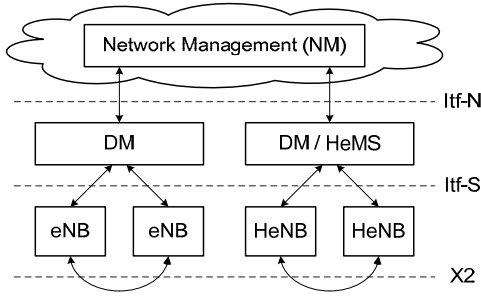


Fig. 3. SON architecture of 3GPP LTE system.

networks. In 3GPP LTE system, automatic parameter configuration and optimization are conducted based on Self Organizing Network (SON) procedures. Fig. 3 illustrates the SON architecture of 3GPP LTE system, where macrocell and femtocell base stations are referred to as Home eNodeB (HeNB) and eNodeB (eNB), respectively [30]. SON algorithms can be implemented either in the end devices, i.e., HeNBs or eNBs, and/or Device Management and/or Home eNodeB Management System, and/or Network Management (NM). However, it is natural that the joint optimization of macrocell and femtocell parameters is performed by NM in a centralized manner, because no direct interface between eNB and HeNB exists. Short-term parameter optimization in the centralized entity, e.g., NM, is almost impossible due to the limited processing power and the limited Operations, Administration and Maintenance bandwidth on the interfaces among the entities. Consequently, the joint parameter optimization involving both macrocells and femtocells need to be performed in the centralized entity at a long-term interval.

Second, short-term resource allocation schemes cannot generally consider the network-wide performance due to the excessive overhead and lack of information. On the other hand, long-term optimization can consider the network-wide performance thanks to the relatively small overhead per unit time and relaxed time constraint. Therefore, our long-term optimization is not incompatible with but complementary to the short-term resource allocation schemes in the sense that the long-term optimization framework can provide good guidelines for the parameter configuration considering the system-wide average performance.

Finally, our long-term parameter selection schemes have the strength in the sense that they can be utilized in both the self-configuration and/or self-optimization phases. Note that SON algorithms can be categorized into self-configuration and self-optimization [6] according to the functionality and phases. Self-configuration presents pre-operational procedures including the initial parameter selection. Though an initial parameter configuration is essential, an initial parameter selection based on the local instantaneous optimization is not generally recommended because the information is very insufficient and unreliable. On the other hand, our algorithm which does not require the instantaneous local information can be used for initial parameter selection. The parameters determined

TABLE III. PATHLOSS PARAMETERS

Environment	Exponent	Fixed loss (dB)
Outdoor	$\alpha_1 = 4$	$Z_1^{\alpha_1} = 30 \log_{10} f_c - 71$
Indoor	$\alpha_2 = 3$	$Z_2^{\alpha_2} = 37$
Outdoor-to-indoor	$\alpha_3 = 4$	$Z_3^{\alpha_3} = 30 \log_{10} f_c - 71 + WL$
Indoor-to-outdoor	$\alpha_4 = 4$	$Z_4^{\alpha_4} = 30 \log_{10} f_c - 71 + WL$
Indoor-to-indoor	$\alpha_5 = 4$	$Z_5^{\alpha_5} = 30 \log_{10} f_c - 71 + 2WL$

by self-configuration may be updated by the localized self-optimization algorithms in the operational phase.

IV. NUMERICAL ANALYSIS OF TWO-TIER CELLULAR NETWORKS

A. Average Throughput of fMS

In this section, we analyze the average throughput performance of fMSs. Let us consider an fMS who is located at r_f away from its serving fBS. As explained in Section III, we simply assume that the distribution of fBSs follows pure SPPP in numerical analysis. Due to the characteristics of homogeneous Poisson point process [26], the interference measured by a typical fMS is representative of the interference seen by all other fMSs. Then, similarly to the SINR models in [31], [32], the complementary cumulative distribution function (CCDF) of an fMS's SINR is given by

$$F_f(\Gamma|r_f) \triangleq \Pr[SINR \geq \Gamma|r_f] \\ = \exp(-sP_N) \exp\left(-\frac{2\pi^2\lambda_f Z_5^{-2}(sP_f)^{2/\alpha_5}}{\alpha_5 \sin(2\pi/\alpha_5)}\right), \quad (9)$$

where $s = \Gamma(Z_2 r_f)^{\alpha_2} P_f^{-1}$. The pathloss parameters in the above equation, i.e., Z_2 , α_2 , Z_5 , and α_5 , are properly chosen from Table III by considering that the fMSs are always located inside the buildings in our system model. The detailed derivation for (9) is given in Appendix A-A.

The probability density of the distance between an fMS and its serving fBS is r_f is given by $\frac{2r_f}{D_h^2}$. Hence, the average spectral efficiency of an fMS, denoted by \bar{B}_f , is calculated as

$$\bar{B}_f = \sum_{l=1}^L \int_0^{D_h} b_l [F_f(\Gamma_l|r_f) - F_f(\Gamma_{l+1}|r_f)] \frac{2r_f}{D_h^2} dr_f, \quad (10)$$

where b_l , Γ_l , and L are the spectral efficiency of rate index l , the SINR threshold to utilize the rate index, and the number of available rate sets, respectively.

At a given average spectral efficiency value, the average throughput of an fMS is degraded when the femtocell resources are shared with other macrocell users i.e., oMSs, in the hybrid (and open) access mode. Let us denote the random variable for the number of oMSs who are associated with an fBS as N_o . Then, the average throughput \bar{T}_f is given by

$$\begin{aligned}\bar{T}_f(\rho, d_f, \beta) &= E[\beta \rho W B_f] + E\left[\frac{(1-\beta)\rho W B_f}{N_o + 1}\right] \\ &= \beta \rho W \bar{B}_f + (1-\beta)\rho W \bar{B}_f E\left[\frac{1}{N_o + 1}\right],\end{aligned}\quad (11)$$

where W is the system bandwidth and B_f is the spectral efficiency of an fMS. In Eq. (11), the dedicated resources to fMS contribute to the first term while the second term is due to the shared resources between fMS and oMS. In addition, the equality holds because the spectral efficiency of an fMS, i.e., \bar{B}_f , is independent of the number of N_o . If we refer to the service area of a given femtocell as y , the number of oMSs in the femtocell's service area follows Poisson random variable with the mean $\lambda_u y$, and the probability mass function (pmf) of $N_o(y)$ is given by

$$f_{N_o(y)}[k] \sim \frac{(\lambda_u y)^k e^{-\lambda_u y}}{k!}, \quad (12)$$

and we obtain the expectation value as

$$E\left[\frac{1}{N_o(y) + 1} \middle| y\right] = \sum_{k=0}^{\infty} \frac{(\lambda_u y)^k e^{-\lambda_u y}}{(k+1)k!} = \frac{1 - e^{-\lambda_u y}}{\lambda_u y}. \quad (13)$$

Let us denote the average service area of a femtocell as $x = E[y]$. From (11) and (13), we obtain the approximated value for the average throughput of an fMS as follows:

$$\begin{aligned}\bar{T}_f(\rho, d_f, \beta) &= \beta \rho W \bar{B}_f + (1-\beta)\rho W \bar{B}_f E_y\left[\frac{1 - e^{-\lambda_u y}}{\lambda_u y}\right] \\ &\cong \beta \rho W \bar{B}_f + \frac{(1-\beta)\rho W \bar{B}_f (1 - e^{-\lambda_u x})}{\lambda_u x}.\end{aligned}\quad (14)$$

The average throughput of an fMS in open access femtocell is obtained by setting $\beta = 0$.

Here, we obtain the average service area, i.e., x , which is a function of the target service radius d_f . A macro user associates with an mBS only when no fBS exists within d_f meters from the user. According to the property of SPPP, the probability that the distance R between a specific mMS and its nearest fBS is larger than r_1 is given by

$$\Pr(R > r_1) = \Pr(\text{No fBS closer than } r_1) = e^{-\pi \lambda_f r_1^2}. \quad (15)$$

Therefore, the probability that a macrocell user is covered by an fBS is given by $1 - e^{-\pi d_f^2 \lambda_f}$, and it is equivalent to the fact that the fBSs cover the area of $A_m(1 - e^{-\pi d_f^2 \lambda_f})$ on average. Because the average number of fBSs in a macrocell area is $A_m \lambda_f$, the average area of a femtocell region can be approximated by

$$x(d_f) = \frac{1 - e^{-\pi d_f^2 \lambda_f}}{\lambda_f}. \quad (16)$$

Because d_f and x have a one-to-one relationship, we use x as the control parameter instead of d_f in the rest of the paper for the simplicity of presentation.

B. Average Throughput of mMMS

In this section, we model the average throughput performance of an mMMS, where mMMS is defined by the macrocell user who is currently associated with the mBS. Let us refer to the distance between an mMMS and its serving mBS as r_m . From the assumption that each fBS fully covers its indoor home area, SINR CCDF of an mMMS for a given r_m is obtained by

$$F_m(\Gamma|r_m) = \exp\left(-\frac{\Gamma(P_N)}{P_m(Z_1 r_m)^{-\alpha_1}}\right). \quad (17)$$

As shown in Table III, Z_1 and α_1 are the fixed pathloss value and the pathloss exponent in outdoor environments, respectively. The detailed derivation for the above equation is shown in Appendix A-B.

The probability that a macrocell user becomes an mMMS, which is referred to as p_{mMS} , is given by

$$p_{mMS} = e^{-\pi \lambda_f d_f^2} = 1 - \lambda_f x, \quad (18)$$

where x is the average service area of a femtocell derived in (16). As shown in (18) that p_{mMS} is independent of the location of the macrocell user, i.e., the distance between the user and the mBS, due to the random distribution of fBSs. Therefore, if we refer to the distance between an mMMS and its serving mBS as r_m , the probability density function (PDF) of r_m is also given by

$$f_{R_m}(r_m) = \frac{2r_m}{D_m^2}. \quad (19)$$

From (17) and (19), the average spectral efficiency of an mMMS is given by

$$\bar{B}_m = \sum_{l=1}^L \int_0^{D_m} b_l [F_m(\Gamma_l|r_m) - F_m(\Gamma_{l+1}|r_m)] \frac{2r_m}{D_m^2} dr_m, \quad (20)$$

where $\Gamma_{L+1} = \infty$. In order to calculate the above equation, we calculate

$$\int_0^{D_m} F_m(\Gamma_l|r_m) r_m dr_m = \int_0^{D_m} r_m e^{-\beta_l r_m^{\alpha_1}} dr_m, \quad (21)$$

where β_l is defined by $P_N \Gamma_l Z_1^{\alpha_1} P_m^{-1}$. By substituting $-\beta_l r_m^{\alpha_1}$ with y , the above equation is obtained by

$$\int_0^{\beta_l D_m^{\alpha_1}} \frac{1}{\alpha_1 \beta_l} \left(\frac{y}{\beta_l}\right)^{\frac{2-\alpha_1}{\alpha_1}} e^{-y} dy = \frac{\beta_l^{-\frac{2}{\alpha_1}}}{\alpha_1} G\left(\frac{2}{\alpha_1}, \beta_l D_m^{\alpha_1}\right), \quad (22)$$

where $G(a, b) \triangleq \int_0^b t^{a-1} e^{-t} dt$ is the incomplete gamma function.

Although femtocell deployment does not change the average spectral efficiency of an mMMS, the average throughput of an mMMS can be improved by deploying the femtocells, because the number of mMMSs sharing the macrocell resource is reduced by relocating some macrocell users, i.e., oMSs, to the femtocells. In our system model, the average number of macrocell users is given by $\bar{N}_u = A_m \lambda_u$. Let us refer to the number of mMMSs in a macrocell area for a given x as N_m . From (18), the

expectation of N_m is given by $\bar{N}_m(x) = A_m \lambda_u (1 - \lambda_f x)$. We approximate N_m as a Poisson random variable with the mean of \bar{N}_m , and hence, the average throughput of an mMS is given by

$$\begin{aligned} \bar{T}_m(\rho, x) &= \sum_{n=1}^{\infty} \frac{(1-\rho) W \bar{B}_m}{n} \frac{n f_{N_m}[n]}{\sum_{k=1}^{\infty} k f_{N_m}[k]} \\ &\cong \frac{(1-\rho) W \bar{B}_m (1 - e^{-A_m \lambda_u (1 - \lambda_f x)})}{A_m \lambda_u (1 - \lambda_f x)}. \end{aligned} \quad (23)$$

C. Average Throughput of oMS

In order to complete the load balancing problem formulated in (3), we analyze the average throughput of an oMSs and the maximum service radius of femtocells, i.e., \bar{T}_o and D_{\max} , respectively. When the target femtocell service radius is configured as d_f , a macrocell user associates with its nearest fBS if the distance between the user and fBS is equal to or smaller than d_f . From (18), the probability that a macrocell user becomes an oMS is given by $\lambda_f x$. Let us refer to the distance between an oMS and its serving fBS as r_o . Then, the conditional probability density function of r_o is given by

$$f_{R_o}(r_o|x) = \begin{cases} \frac{2\pi\lambda_f r_o e^{-\pi\lambda_f r_o^2}}{\lambda_f x}, & 0 \leq r_o \leq \sqrt{\frac{\ln(1-\lambda_f x)}{-\pi\lambda_f}}, \\ 0, & \text{otherwise.} \end{cases} \quad (24)$$

When r_o is given, the SINR CCDF of an oMS is given by:

$$\begin{aligned} F_o(\Gamma|r_o) &= \exp\left(-\frac{\pi\lambda_f \sqrt{sP_f}}{Z_f^2} \left(\frac{\pi}{2} - \tan^{-1}\left(\frac{Z_f^2 r_o^2}{\sqrt{sP_f}}\right)\right) - sP_N\right), \end{aligned} \quad (25)$$

where

$$(Z_I, s) = \begin{cases} \left(Z_4, P_f^{-1} \Gamma (Z_4 r_o)^{\alpha_4}\right), & r_o \geq D_h, \\ \left(Z_5, P_f^{-1} \Gamma (Z_2 r_o)^{\alpha_2}\right), & \text{otherwise.} \end{cases} \quad (26)$$

The detailed derivation for the above equation is found in Appendix A-C.

Then, we obtain the average spectral efficiency of an oMS. If we refer to the probability that an oMS chooses the rate index l as $f_L[l|r_o] = F_o(\Gamma_l|r_o) - F_o(\Gamma_{l+1}|r_o)$, the average spectral efficiency of an oMS is given by

$$\bar{B}_o(x) = \sum_{l=1}^L \int_0^{d_f(x)} b_l f_L[l|r_o] f_{R_o}(r_o|x) dr_o, \quad (27)$$

where $f_{R_o}(r_o|x)$ is shown in (24).

We refer to the random variable representing the number of oMSs in a femtocell area as N_o . As done for the average throughput analysis of an fMS in (14), we approximately assume that N_o is a Poisson random variable with the mean of $\lambda_u x$. Because $N_o + 1$ users including an fMS equally share the femtocell resources in the open access mode and only $1 - \beta$

fraction of intra-femtocell resources are allowed to the oMSs, the average throughput of oMSs is expressed by

$$\bar{T}_o(\rho, x, \beta) = \sum_{n_o=1}^{\infty} \frac{\rho(1-\beta) W \bar{B}_o(x)}{n_o + 1} \frac{n_o f_{N_o}[n_o]}{\sum_{k=1}^{\infty} k f_{N_o}[k]}, \quad (28)$$

where

$$\sum_{n=1}^{\infty} \frac{n f_{N_o}[n]}{n+1} = \frac{1}{\bar{N}_o} \sum_{n=2}^{\infty} (n-1) \frac{\bar{N}_o^n e^{-\bar{N}_o}}{n!} = \frac{\lambda_u x + e^{-\lambda_u x} - 1}{\lambda_u x}. \quad (29)$$

From (28) and (29), \bar{T}_o is obtained by

$$\bar{T}_o(\rho, x, \beta) = \frac{(1-\beta) \rho W \bar{B}_o(x) (\lambda_u x + e^{-\lambda_u x} - 1)}{(\lambda_u x)^2}. \quad (30)$$

Furthermore, we analyze the maximum service radius of a femtocell, i.e., D_{\max} , to complete the problem formulation in (3). D_{\max} is an important parameter which determines the range of our design parameter d_f (or x). As described in Section III-B, we define D_{\max} as the maximum target service radius where the average outage rate of an oMS is less than or equal to O_{\max} . We assume that an outage occurs when the instantaneous SINR is less than the threshold for the lowest transmission rate, i.e., Γ_1 in Table I. From the definition, average outage rate of an oMS with the given target service radius d_f is calculated by

$$\bar{O}_o(d_f) = \int_0^{d_f} (1 - F_o(\Gamma_1|r_o)) f_{R_o}(r_o|d_f) dr_o, \quad (31)$$

which looks very similar to (27). D_{\max} is obtained from the equation $\bar{O}_o(D_{\max}) = O_{\max}$. Though D_{\max} cannot be given in a closed form, the near-optimal solution for (31) can easily be obtained by using the simple binary search algorithm because $\bar{O}_o(d_f)$ is a monotonically increasing function of d_f . Because any mobile stations which are in the femtocell coverage should attached to femtocell, SINR of the oMS is likely to worse as the service radius of a femtocell, d_f , is larger when it is larger than threshold, i.e., the radius that a reference signal received power from the nearest fBS and mBS are about the same. The detailed description for the binary search algorithm is omitted due to the space limitation.

V. OPTIMIZATION IN OPEN ACCESS FEMTOCELL NETWORKS

A. Optimization of Parameters in Open Access Femtocell Networks

In this section, we prove that our optimization problem in open access mode becomes a single variable convex problem in some typical environments, and the optimal parameters are obtained. In this section, $\beta = 0$ because we consider the open access femtocells. If we define $\bar{t}_m(x)$ and $\bar{t}_{fo}(x)$ as

$$\bar{t}_m(x) = \frac{\bar{T}_m(\rho, x, \beta = 0)}{W(1-\rho)} \quad (32)$$

and

$$\bar{t}_{fo}(x) = \min \left(\frac{\bar{T}_f(\rho, x, \beta = 0)}{MW\rho}, \frac{\bar{T}_o(\rho, x, \beta = 0)}{KW\rho} \right) \quad (33)$$

the optimization problem (3) is rephrased by

$$\max_{(\rho, x)} (1 - \rho) \bar{t}_m(x) \quad (34)$$

s.t.

$$\rho \bar{t}_{fo}(x) \geq (1 - \rho) \bar{t}_m(x), \quad (35)$$

$$X_{\min} \leq x \leq X_{\max}, \quad (36)$$

$$0 \leq \rho \leq 1, \quad (37)$$

where $X_{\min} = x(D_h)$ and $X_{\max} = x(D_{\max})$ from (16).

Proposition 1: The optimal ρ^* which maximizes the objective in (34) is given by $\rho^* = \frac{\bar{t}_m(x^*)}{\bar{t}_{fo}(x^*) + \bar{t}_m(x^*)}$, where x^* is the optimal value of x .

Proof: See Appendix B-A. ■

As inferred by (33) and (35), the performance of our load balancing algorithm is always limited by the throughput requirement of an fMS if $K\bar{T}_f(\rho, x, 1) \leq M\bar{T}_o(\rho, x, 1)$ for all $x \in [X_{\min}, X_{\max}]$. We define such cases by the fMS's requirement-limited environments. Then, the following proposition holds.

Proposition 2: In the fMS's requirement-limited environments, the optimization problem (34) is a convex optimization problem.

Proof: See Appendix B-B. ■

From the above proposition, the optimal solution of x can be efficiently obtained by using the standard methods used for solving the convex optimization [33] if the given environment is the fMS's requirement-limited environment. We expect that the two-tier cellular networks mostly operate in the fMS's requirement-limited environments, because the oMS's throughput requirement is easily satisfied with the reasonably large fMS's benefit requirement, i.e., M . However, if the given environment is not the fMS's requirement-limited environment, we should obtain the near-optimal solution of x using the inefficient exhaustive search algorithm. To check whether a given environment is the fMS's requirement-limited environment, the following proposition could be useful.

Proposition 3: If we define $C(x) \triangleq \frac{(1 - e^{-\lambda_u x})}{\lambda_u x}$ and $D(x) \triangleq \frac{(\lambda_u x + e^{-\lambda_u x} - 1)}{(\lambda_u x)^2}$, $\frac{\bar{B}_f C(X_{\min})}{\bar{B}_o(X_{\max}) D(X_{\min})} \leq \frac{M}{K}$ is the sufficient condition that a given environment is the fMS's requirement-limited environment.

Proof: See Appendix B-C. ■

From the (near) optimal value x^* , the service area control is implemented by setting P_{cs} according to (2) and (16). The optimal ρ^* is configured according to Proposition 1.

The optimal solution x^* has the following property.

Proposition 4: $\frac{\bar{N}_f \bar{B}_f}{M \bar{B}_o} > 1$, where \bar{N}_f is the average number of fBSs in a macrocell area, is a sufficient condition that the optimal solution of the problem (34) is given by $x^* = X_{\max}$ in the typical fMS's requirement limited environments where the average number of users in a macrocell is larger than that in a single femtocell.

Proof: See Appendix B-D. ■

Proposition 4 can be interpreted as follows. The expansion of the femtocell service area is encouraged if the average spectral efficiency of an fMS is much larger than that of an mMS, and the expansion of the femtocell service area is also encouraged if there are many femtocells in the system because the sum of performance gain in the system is approximately proportional to the number of femtocells. On the other hand, large benefit requirements from fMSs, i.e., M , can limit the service area expansion to guarantee the performance of femtocell owners who are the premium users.

B. Extension Considering Interference Thinning (Thin)

As described in Proposition 4, the optimal performance of our load balancing scheme is determined by the physical limitation D_{\max} in many cases. Therefore, we expect that the efficiency of our load balancing scheme can be enhanced if the maximum coverage of femtocell is increased by applying an interference thinning scheme, which reduces the interference by limiting the resource usage in fBSs while all the BSs fully utilize the given resources in our basic model. In our interference thinning scheme, the probability that an fBS uses a specific resource block is limited to θ , to reduce the interference among femtocells. The channel condition is improved by using $\theta < 1$, but using small θ can reduce the aggregate throughput by decreasing chances for packet transmissions. Our proposed scheme including the interference thinning scheme is referred to as OA-Thin. The objective and constraints of OA-Thin is the same as those of the original problem formulation in OA scheme, but we optimize the new control parameter, i.e., θ , as well as ρ and d_f to maximize our objective while satisfying the constraints.

Some parameters in our analytic model are updated by considering θ . The SINR distribution of an fMS and an oMS, i.e., $F_f(\Gamma|r_m)$ in (9) and $F_o(\Gamma|r_o)$ in (25), are updated by replacing λ_f in the equations with $\theta\lambda_f$. Furthermore, D_{\max} in is also updated considering θ .

It is difficult to show that finding the optimal solution of OA-Thin scheme is a convex problem in the fMS's requirement-limited environments as described in Proposition 2. However, if θ is given, Proposition 2 holds, and we can find the optimal $x^*(\theta)$ and $\rho^*(\theta)$ efficiently in the typical environments where the operation is dominated by the benefit requirement of fMSs. Therefore, we repeatedly solve the convex optimization problems with various candidate θ values, and θ which minimizes the objective function is chosen as the suboptimal θ^* .

C. Analysis of Optimal Parameters

In this section, we show the optimal parameters of the proposed schemes based on our analytic model. The basic parameters shown in Table II are used in the evaluations unless mentioned otherwise, and we obtain the results with various M values, where fMSs require M times higher average throughput than the average throughput of mMS.

Fig. 4(a) shows the optimal service radius d_f^* given by the optimization of OA and OA-Thin schemes. The straight lines

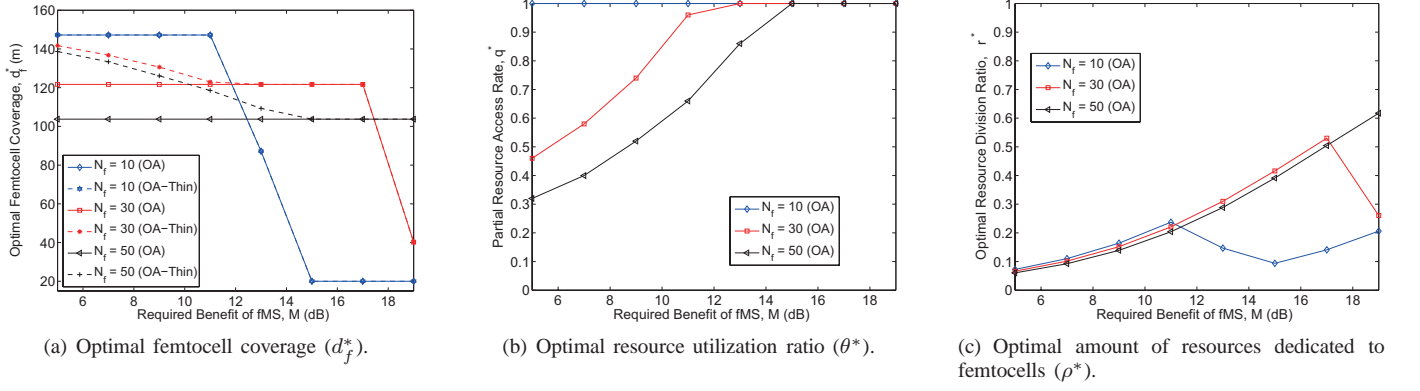


Fig. 4. Optimal parameters.

in the figure represent D_{\max} with the given average number of fBSs which is referred to as \bar{N}_f . As \bar{N}_f increases, D_{\max} value decreases due to the increased interference. For all \bar{N}_f values, OA scheme determines to use D_{\max} as the service radius of femtocells when M is not very large. If M exceeds some threshold, the optimal femtocell radius becomes smaller than D_{\max} , because sharing the femtocell resources with many oMSs is not an efficient method to provide a large relative benefit to the fMSs. In the sense of \bar{N}_f , D_{\max} is preferred in the wider range of M values when \bar{N}_f is large, because the offloading gain of using femtocells is more significant with the large number of fBSs. These results are the same results which are inferred by Proposition 4.

The optimal resource utilization ratio of femtocells, i.e., θ^* , in OA-Thin scheme is shown in Fig. 4(b). The needs for interference management is larger in the environments where many fBSs exist. Therefore, Fig. 4(a) shows that OA-Thin scheme chooses to expanding the maximum service radius by applying $\theta < 1$ when there are 30 or 50 fBSs in average. In the mean time, the interference thinning is not effective when M is very large, because it is difficult to satisfy the requirement of M if fBSs use the partial resources in the femtocells. Accordingly, Fig. 4(b) shows that the femtocells are required to fully utilize the dedicated femtocell resources when M is large.

The optimal ratio of resources dedicated to femtocells, i.e., ρ^* , is shown in Fig. 4(c). For the region where d_f^* is fixed, ρ^* proportionally increases as M increases. However, in the middle region where d_f^* increases, ρ^* decreases to properly maximize the average throughput of mMSs while meeting the requirements for the fMS's performance.

VI. OPTIMIZATION IN HYBRID ACCESS FEMTOCELL NETWORKS

In hybrid access femtocell networks, we optimize β as well as x and ρ . The analysis results for the open access femtocell networks in the previous section are used in the optimization procedures for the hybrid access femtocell networks.

Proposition 5: When the target femtocell service area x is given, the optimal ρ^* and β^* which maximize the objective in

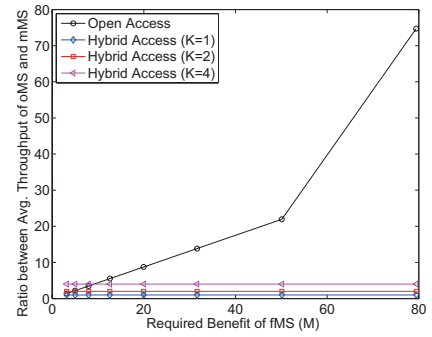


Fig. 5. Ratio between the average throughputs of oMS and mMS.

(3) are given as follows:

$$\beta^*(x) = \begin{cases} \frac{-C(x)+D(x)}{B(x)-C(x)+D(x)}, & D(x) \geq C(x), \\ 0, & \text{otherwise,} \end{cases} \quad (38)$$

and

$$\rho^*(x) = \begin{cases} \frac{\frac{A(x)}{B(x)-C(x)+D(x)} + A(x)}{\frac{A(x)}{D(x)+A(x)}}, & D(x) \geq C(x), \\ \frac{A(x)}{D(x)+A(x)}, & \text{otherwise,} \end{cases} \quad (39)$$

where $A(x) \triangleq \frac{\bar{B}_m(1-e^{-A_m\lambda_u(1-\lambda_f x)})}{A_m\lambda_u(1-\lambda_f x)}$, $B(x) \triangleq \frac{\bar{B}_f}{M}$, $C(x) \triangleq \frac{\bar{B}_f(1-e^{-\lambda_u x})}{M\lambda_u x}$, and $D(x) \triangleq \frac{\bar{B}_o(x)(\lambda_u x + e^{-\lambda_u x} - 1)}{K(\lambda_u x)^2}$.

Proof: See Appendix B-E. \blacksquare

From Proposition 5 and the original problem formulation in (3), the load balancing problem in hybrid access femtocell can be treated as the single variable optimization with the control parameter x . Unfortunately, the above optimization problem is not a convex optimization problem. Therefore, we find a near-optimal solution by calculating the objective function over the feasible region of x . Because the original problem has been simplified to a single variable problem and the feasible region of x is bounded, we can find the near-optimal solution x^* without excessively complex computations.

The performance gain of mMMS and fMS in the hybrid access femtocell networks is achieved at the cost of the average performance degradation of an oMS by using $\beta > 0$. Fig. 5 describes the ratio between the throughputs of oMSs and mMMSs in open access femtocells and hybrid access femtocells based on analysis. oMSs in the open access femtocells enjoy much larger throughput performance than oMSs in the hybrid access femtocells thanks to the resource-fair intra scheduling of the fBS. However, it is unfair that the oMSs achieve such large throughput because the oMSs and mMMSs are actually the same type of users who do not pay any cost for the femtocell deployment. On the other hand, the hybrid access fBS distinguishes the fMS from the oMSs and the average throughput of oMSs are properly controlled so that the similar quality of services are provided to the mMMSs and oMSs. Fig. 5 shows that the average throughput of an oMS in the hybrid access femtocell networks is exactly K times larger than that of an mMMS, where K is generally a small value.

VII. PERFORMANCE EVALUATION

A. Evaluation Environments and Comparing Schemes

In this section, we evaluate our proposed schemes based on both numerical analysis and computer simulations. As described in Section III, macrocell users and fBSs are randomly deployed according to SPPP, while one constraint that the distance between the fBSs should be less than $2D_h$ is additionally given in the simulation settings. The channel model used for the numerical analysis and simulation is described in Section III, and the basic values of the evaluation parameters are provided in Table II [12], [34]. We consider the random mobility of macrocell users in the simulations, and the performances of users located in the interested area, i.e., a single macrocell area, are considered for the performance analysis.

In our evaluations, the proposed schemes are compared with some comparing schemes. The basic comparing scheme is CoRSSI where the mBSs and fBSs share the same bandwidth, and a user associates with the cell which provides the best signal strength including both macrocells and femtocells. CoRSSI is excellent in the aspect of sum capacity by fully reusing the bandwidth, but the benefit achieved by mMMS can be smaller than the dedicated bandwidth based schemes due to the limited offloading gain as will be shown in Section VII-B. In order to show the maximum offloading gain in a co-channel deployment, we also introduce CoLB (Cochannel Load Balancing) scheme where the system promotes the users to access femtocell as much as possible while the basic requirement for service coverage of femtocell is satisfied. The details of CoLB is described in Section VII-B. DivRSSI is the scheme which assigns the dedicated orthogonal resources to femtocells like the proposed schemes, and each MS associates with the BS which provides the best RSSI value like CoRSSI. In DivRSSI, the bandwidth is divided into the macro and femtocell resources with the optimal ratio, i.e., ρ^* , while maintaining the constraints $\bar{T}_f \geq M\bar{T}_m$ and $\bar{T}_f \geq K\bar{T}_o$. The optimal ρ^* is chosen based on the simulation results in DivRSSI because no numerical analysis model exists for

DivRSSI. Finally, femtocells do not allow any open or hybrid access of oMSs to access femtocells in CoCA and DivCA, where CA stands for Closed Access. Similarly to DivRSSI, the optimal bandwidth dedicated to femtocell is applied for DivCA based on the simulation results, while the whole resources are shared by macrocell and femtocell users in CoCA.

B. Analysis and Simulation Results

In this section, we evaluate the performance of proposed schemes using numerical analysis. The default evaluation parameters specified in Table II are used unless mentioned otherwise. First, we show that the numerical analysis is valid in spite of the simplifying assumptions and approximations in the numerical analysis. We obtain the average spectral efficiency and average throughput of an fMS, oMS, and mMMS when the service radius d_f values are given. After simulations with 10,000 distributions, we compare the average simulation results with the analysis result as shown in Fig. 6(a). The validation results indicate that the errors between the results of the numerical analysis and computer simulation are negligible, i.e., less than 1 %.

Fig. 6(b) shows the average throughput of an mMMS. We find that the performance of mMMSs is enhanced by utilizing the proposed schemes in most regions. When the required benefit from fMSs is small, the more aggressive traffic offloading from macrocell users is feasible. Therefore, the performance gains of OA and OA-Thin are more significant when M is small. Among the comparing schemes CoRSSI provides comparable or even better average throughput performance to mMMSs than the proposed schemes when the required fMS's benefit exceeds a certain value. This result shows that co-channel deployment could be more efficient to guarantee very large performance benefits to fMSs. However, this phenomenon happens when M is very large, e.g., $M > 50$ in this example, and such large benefits for fMSs might not be required in reality. HA(-Thin) schemes achieve the better average throughput of an mMMS than OA(-Thin) schemes. Especially, the gain of hybrid access femtocell is still very significant even in the environments where M is very large, while the open access femtocell's offloading gain is limited in the environments. In HA(-Thin) schemes, the performance of mMMSs and fMSs are improved by preventing the oMSs from achieving the performance gain much more than necessary. OA-Thin and HA-Thin schemes obtain the further performance gain by improving the SINR status and extending the maximum femtocell coverage. As discussed in Section V-C, the partial utilization of femtocell resources, i.e., OA/HA-Thin, is preferred when M is small.

The impact of the number of fBSs in a macrocell area is shown in Fig. 6(c). In the open access femtocell networks, the performance of mMMS is enhanced as the number of fBSs increases because the chances for the offloading of macrocell's traffic increases. As the previous propositions implicate, the interference thinning in OA/HA-Thin becomes useful when the number of fBSs is large where the load balancing efficiency is maximized. Obviously, the performance of CoCA scheme, i.e., co-channel deployment based on the closed access femtocells, is rapidly degraded as N_f increases due to the excessive co-channel interference.

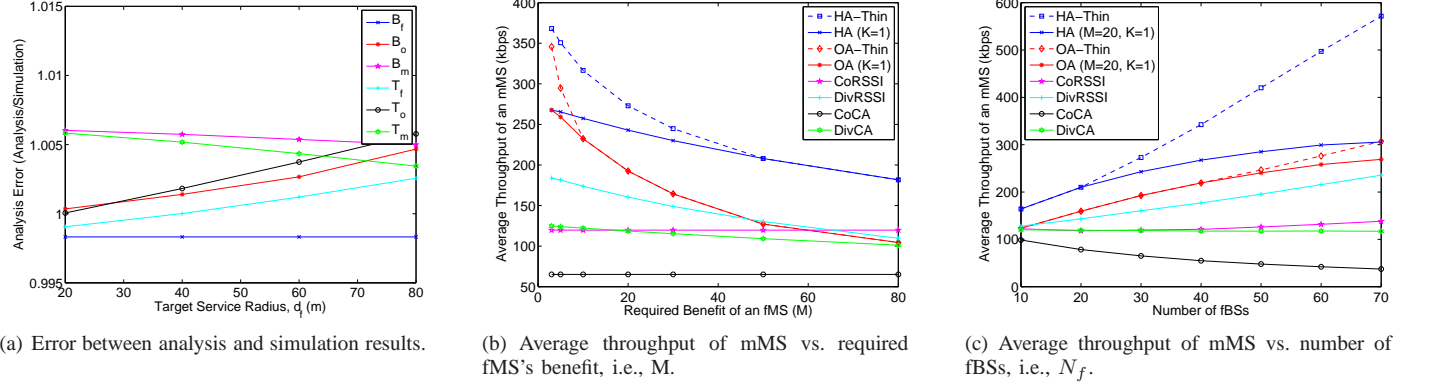
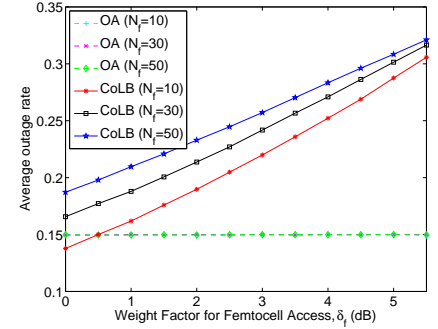


Fig. 6. Basic simulation results.

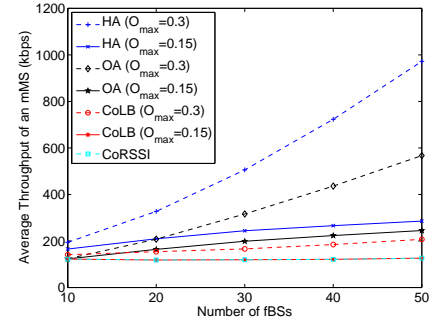
Load balancing gain can also be enhanced in co-channel deployment scenario by expanding the service coverage of femtocells. CoLB scheme expands the service coverage of femtocells as much as possible while the basic requirement for signal quality is satisfied. A weight factor for femto-cell access, i.e., δ_f , is notified by the system under CoLB scheme, and a macrocell user associates with a femtocell if $\delta_f RSSI_{f,\max} > RSSI_m$, where $RSSI_{f,\max}$ is the maximum received signal strength from the nearby fBSs and $RSSI_m$ is the received signal strength from the mBS, respectively. CoLB is identical to CoRSSI when $\delta_f = 1$. Though the offloading gain obtained in the macrocell tier increases as δ_f increases, the maximum δ_f is limited by the service quality constraint, e.g., average outage rate, of oMSs. For a fair comparison with the proposed schemes, we use the maximum δ_f which satisfies $\bar{O}_o(\delta_f) \leq O_{\max}$, where the outage rate threshold, i.e., O_{\max} , is the same as that used in the proposed schemes to limit the maximum femtocell service radius, i.e., D_{\max} .

Fig. 7(a) shows the average outage rate of oMSs when δ_f is given. As shown in the figure, the average outage rate of oMSs increases as δ_f increases. In our evaluation environments, CoLB cannot expand the service coverage when the number of fBSs is 30 or 50 because the average outage rate exceeds the configured threshold, i.e., $O_{\max} = 0.15$, even when δ_f is 0 dB. A small margin for coverage expansion is available when the number of fBSs is 10. On the other hand, the proposed scheme adaptively manages the average outage rate according to the number of fBSs.

Fig. 7(b) shows the average throughput of mMBS when the optimal δ_f is applied to CoLB. To give more flexibility to coverage control, we consider a relaxed coverage requirement where $O_{\max} = 0.3$ as well as the basic requirement, i.e., $O_{\max} = 0.15$. With $O_{\max} = 0.15$, the performance of CoLB is very close to that of CoRSSI due to the limited offloading gain, and only a small performance gain is observed when the number of fBSs is 10. On the other hand, a significant performance gain is provided to mMBS with the proposed schemes. When a relaxed average outage requirement is applied, i.e., $O_{\max} = 0.3$, CoLB achieves a larger mMBS throughput than CoRSSI for most cases at the cost of increased outage rate.



(a) Average outage rate of oMS in CoLB scheme.



(b) Average throughput of mMBS using CoLB scheme.

Fig. 7. Performance of CoLB scheme

However, the performance gains of mMBSs achieved by the proposed schemes in the relaxed outage requirement are much more significant than the one achieved by CoLB. Note that this result does not mean that the proposed scheme is always better than the co-channel based schemes. The proposed schemes have strength in improving the performance of mMBSs while limiting the relative benefits of fMSs and oMSs around the planned levels. On the other hand, in the aspect of the total system capacity, the co-channel based scheme is more efficient. Therefore, the choice of the resource management should be adaptive to various aspects, e.g., the system environments,

status of market, consumer's characteristics, mobile operator's policy, and so on.

C. Impact of Other Environmental Parameters

Our basic system model used in the previous sections includes some simplifying assumptions, e.g., uniform user distribution, to ensure the numerical tractability. The numerical analysis and optimization are important in spite of the simplification because it gives the intuition for the system performance and optimal parameters. However, investigation for realistic environments would be beneficial for further understandings. In this section, we consider some more environmental parameters which have not been considered in the basic numerical model, and the impacts of the new environmental parameters are analyzed through the simulations.

We assume the uniform user distribution in the basic model, but it is generally said that indoor user density is much larger than outdoor. Therefore, we introduce new environmental parameter to represent the heterogeneity for indoor and outdoor user densities, i.e., k_{in} . We refer to the outdoor and indoor user densities as $\lambda_{u,o}$ and $\lambda_{u,i} = k_{in}\lambda_{u,o}$, respectively. Then, the average number of mMSSs is obtained by

$$\bar{N}_m = (A_m - \lambda_f A_m x) \lambda_{u,o}, \quad (40)$$

and the average number of oMSSs in a femtocell area is given by

$$\bar{N}_o = k_{in} \lambda_{u,o} x (D_h) + \lambda_{u,o} (x - x(D_h)), \quad (41)$$

where $x(D_h) = \frac{1 - e^{-\pi D_h^2 \lambda_f}}{\lambda_f}$ from (16). By putting (40) and (41) into the analysis in Section IV, the performance of the proposed schemes with a heterogeneous user distribution can be numerically analyzed.

Fig. 8(a) shows the average throughput of mMSS with a heterogeneous user distribution. As shown in Fig. 8(a), the load balancing gain of all the open access schemes increase as the indoor user density increases because indoor femtocells can efficiently offload the traffic of the indoor users. The relative gain of OA scheme is reduced when the indoor user density is high, because the comparing schemes also enjoy high offloading gain from indoor macrocell users. On the other hand, HA scheme still maintains the relative gain for mMSS by limiting the performance of oMSSs.

In the real environments, the maximum number of users served in a single femtocell is limited due to the capability of the cheap femtocell device. We refer to the maximum number of users instantaneously allowed to access a femtocell as N_{max} . We investigate the impact of N_{max} using simulations. In the simulations, each macrocell user is dropped in a random location, and it first tries to choose the best femtocell or macrocell based on the criterion of the employed target cell selection scheme. If the target cell is a femtocell and the number of users in the cell already exceeds N_{max} , then the user tries to choose the next best cell according to the cell selection criterion. Multiple simulations are conducted for the quantized target femtocell service area candidates, i.e., x . Then, the optimal bandwidth division ratio and intra-femtocell resource dedicated ratio at a given x , i.e., $\rho^*(x)$ and $\beta^*(x)$, are

numerically obtained by using Proposition 1 and Proposition 5. Finally, the near optimal x^* is chosen by comparing the results for various x values.

Fig. 8(b) shows the average throughput of an mMSS when the number of admissible users is limited by a specified value. If only a small number of users can be served by an fBS, the average throughput of an mMSS cannot be enhanced much although the load balancing schemes are used. In our evaluation environments, the offloading gain sharply decreases when the number of admissible users is less than 6. On the other hand, if the number of admitted users is larger than 8, the performance enhancement is almost saturated.

Our basic assumption for femtocell distribution is that the buildings (or houses) are randomly distributed according to SPPP. In order to show the performance in the realistic environments, we show the simulation results based on the real deployment information for WiFi APs. Because the femtocell service is in an early phase, we use the location information of WiFi APs registered in [35], where we assume that some of the WiFi APs are replaced by femtocells.

Simulation results shown in Fig. 8(c) have been obtained based on the deployment information around the Seoul station, which is the downtown of Seoul, Korea. In order to compare the results with the basic results in Section VII-B, we assume that only the predefined ratio of WiFi APs in the area are replaced by femtocells, and the density of the femtocell in the macrocell area is known to the system. We obtain the averaged value after 300 simulations where different randomly chosen WiFi APs' locations are assumed in each simulation run. The same channel model which is used in the numerical analysis is used for the simulations. The meaning of this simulation result may be limited because the performance gap between the numerical analysis and real performance results is severely affected by the system environment. However, the simulation results in Fig. 8(c) shows that analysis results show similar trends to the simulation in some cases, and the proposed schemes still have performance gain even though the optimization based on the local information has not been performed. Although the analysis results can be different from the performance in the real system, the numerical analysis and optimization are still very important because it can give the insights for the network performance in the various environments and good guidelines for the system design.

VIII. CONCLUSION

In this paper, we develop the load balancing schemes which are efficient in the environments where the open or hybrid access femtocells coexist with the macrocells. We aim at maximizing the average throughput performance of mMSS while guaranteeing some amount of benefits to the fMSSs who deploy femtocells in their homes. In order to maximize the offloading gain of the open and hybrid access femtocells, we propose to use the separate bandwidth deployment, and we jointly optimize the effective service areas of femtocells and the amount of dedicated resources for femtocells. Using the analytic model, we prove that the joint optimization problem is a convex optimization problem in some typical environments.

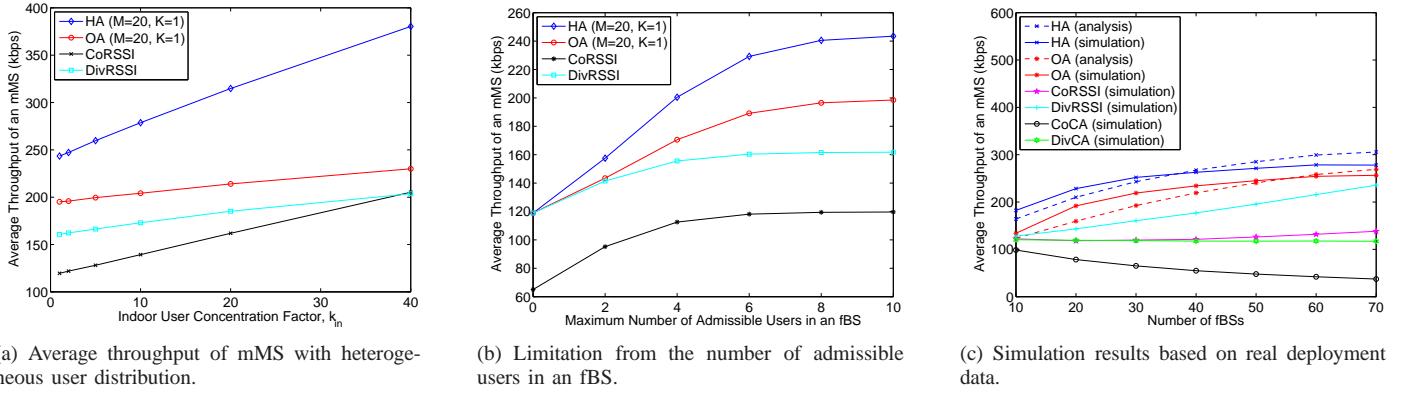


Fig. 8. Impact of Other Environmental Parameters.

We also introduce the scheme which applies the interference thinning scheme on top of the proposed schemes in order to further enhance the offloading gain. In the hybrid access femtocells, the performance of our load balancing scheme is improved by optimally determining the amount of dedicated resources only for the fMSs. Performance evaluation results show that the proposed schemes significantly improve the system-wide performance while satisfying the requirements of fMSs.

REFERENCES

- [1] J. Andrews, H. Clausen, M. Doherty, S. Rangan, and M. Reed, "Femtocells: Past, Present and Future," *IEEE Journal on Selected Areas of Communications*, vol. 30, pp. 497–508, Apr. 2012.
- [2] D. Lopez-Perez, A. Valcarlos, G. de la Roche, and J. Zhang, "Access Methods to WiMAX Femtocells: A Downlink System-Level Case Study," in *Proc. IEEE ICCS*, Baton Rouge, USA, Nov. 2009.
- [3] P. Xia, V. Chandrasekhar, and J. G. Andrews, "Femtocell Access Control in the TDMA/OFDMA Uplink," in *Proc. IEEE Globecom*, Miami, USA, Dec. 2010.
- [4] H.-S. Jo, P. Xia, and J. G. Andrews, "Downlink Femtocell Networks: Open or Closed?" in *Proc. IEEE ICC*, Kyoto, Japan, Jun. 2011.
- [5] 3GPP TS 36.300 v8.12.0, *Technical Specification Group Radio Access Network; Evolved Universal Terrestrial Radio Access (E-UTRA) and Evolved Universal Terrestrial Radio Access Network (E-UTRAN); Overall description; Stage 2 (Release 8)*, 3GPP, Dec. 2010.
- [6] 3GPP TS 36.300 v9.0.0, *Technical Specification Group Radio Access Network; Evolved Universal Terrestrial Radio Access (E-UTRA) and Evolved Universal Terrestrial Radio Access Network (E-UTRAN); Overall description; Stage 2 (Release 9)*, 3GPP, Dec. 2011.
- [7] I. Guvenç, M.-R. Jeong, F. Watanabe, and H. Inamura, "Hybrid Frequency Assignment for Femtocells and Coverage Area Analysis for Co-Channel Operation," *IEEE Commun. Lett.*, vol. 12, pp. 880–882, Dec. 2008.
- [8] D. Choi, P. Monajemi, S. Kang, and J. Villaseñor, "Dealing with Loud Neighbors: The Benefits and Tradeoffs of Adaptive Femtocell Access," in *Proc. IEEE Globecom*, New Orleans, USA, Nov. 2008.
- [9] H. Clausen and F. Pivert, "Femtocell Coverage Optimization using Switched Multi-element Antennas," in *Proc. IEEE ICC*, Dresden, Germany, Jun. 2009.
- [10] K. Sundaresan and S. Rangarajan, "Efficient Resource Management in OFDMA Femto Cells," in *Proc. ACM MobiHoc*, New Orleans, USA, May 2009.
- [11] Y. Bai, J. Zhou, and L. Chen, "Hybrid Spectrum Usage for Overlaying LTE Macrocell and Femtocell," in *Proc. IEEE Globecom*, Honolulu, USA, Nov. 2009.
- [12] H.-S. Jo, C. Mun, J. Moon, and J.-G. Yook, "Self-Optimized Coverage Coordination in Femtocell Networks," *IEEE Trans. Wireless Commun.*, vol. 9, no. 10, pp. 2977–2982, Oct. 2010.
- [13] S. Kaimaletu, R. Krishnan, S. Kalyani, N. Akhtar, and B. Ramamurthi, "Cognitive Interference Management in Heterogeneous Femto-Macro Cell Networks," in *Proc. IEEE ICC*, Kyoto, Japan, Jun. 2011.
- [14] S. Park and S. Bahk, "Dynamic Inter-Cell Interference Avoidance in Self-Organizing Femtocell Networks," in *Proc. IEEE ICC*, Kyoto, Japan, Jun. 2011.
- [15] M. Y. Arslan, J. Yoon, K. Sundaresan, S. V. Krishnamurthy, and S. Banerjee, "FERMI: A Femtocell Resource Management System for Interference Mitigation in OFDMA Networks," in *Proc. ACM MobiCom*, Las Vegas, USA, Sep. 2011.
- [16] A. Hatoum, N. Aitsaadi, R. Langar, R. Boutaba, and G. Pujolle, "FCRA: Femtocell Cluster-based Resource Allocation Scheme for OFDMA Networks," in *Proc. IEEE ICC*, Kyoto, Japan, Jun. 2011.
- [17] K. Han, Y. Choi, M. Na, D. Kim, S. Choi, and K. Han, "Optimization of Femtocell Network Configuration under Interference Constraints," in *Proc. WiOpt*, Seoul, Korea, Jun. 2009.
- [18] J. Kim and D.-H. Cho, "A Joint Power and Subchannel Allocation Scheme Maximizing System Capacity in Dense Femtocell Downlink Systems," in *Proc. IEEE PIMRC*, Tokyo, Japan, Sep. 2009.
- [19] S.-M. Cheng, W. C. Ao, and K.-C. Chen, "Efficiency of a Cognitive Radio Link with Opportunistic Interference Mitigation," *IEEE Trans. Wireless Commun.*, vol. 10, no. 6, pp. 1715–1720, Jun. 2011.
- [20] M. Bennis and M. Debbah, "On Spectrum Sharing with Underlaid Femtocell Networks," in *Proc. IEEE PIMRC*, Istanbul, Turkey, Sep. 2010.
- [21] J.-S. Lin and K.-T. Feng, "Game Theoretical Model and Existence of Win-Win Situation for Femtocell Networks," in *Proc. IEEE ICC*, Kyoto, Japan, Jun. 2011.
- [22] M. Bennis and S. M. Perlaza, "Decentralized Cross-Tier Interference Mitigation in Cognitive Femtocell Networks," in *Proc. IEEE ICC*, Kyoto, Japan, Jun. 2011.
- [23] C.-H. Ko and H.-Y. Wei, "On-Demand Resource-Sharing Mechanism Design in Two-Tier OFDMA Femtocell Networks," *IEEE Trans. Veh. Technol.*, vol. 60, pp. 1059–1071, Mar. 2011.
- [24] V. Chandrasekhar and J. G. Andrews, "Spectrum Allocation in Tiered Cellular Networks," *IEEE Trans. Commun.*, vol. 57, pp. 3059–3068, Oct. 2009.
- [25] V. Chandrasekhar, M. Kountouris, and J. G. Andrews, "Coverage in Multi-Antenna Two-Tier Networks," *IEEE Trans. Wireless Commun.*, vol. 8, no. 10, pp. 5314–5327, Oct. 2009.

- [26] J. Kingman, *Poisson Processes*, 1st ed. Oxford University Press, 1993.
- [27] KOSTAT: Statistics Korea (2010), <http://kosis.kr/eng>.
- [28] United States Census Bureau (2012), <http://www.census.gov>.
- [29] A. J. Goldsmith and S.-G. Chua, "Variable-Rate Variable-Power MQAM for Fading Channels," *IEEE Trans. Commun.*, vol. 45, pp. 1218–1230, Oct. 1997.
- [30] S. Hamalainen, H. Sanneck, and C. Sartori, *LTE Self Organising Networks (SON)*, 1st ed. Wiley, 2012.
- [31] F. Baccelli, B. Blaszczyzyn, and P. Muhlethaler, "An Aloha Protocol for Multihop Mobile Wireless Networks," *IEEE Trans. Inform. Theory*, vol. 52, no. 2, pp. 421–436, Feb. 2006.
- [32] S.-M. Cheng, W. C. Ao, and K.-C. Chen, "Downlink Capacity of Two-tier Cognitive Femto Networks," in *Proc. IEEE PIMRC*, Istanbul, Turkey, Sep. 2010.
- [33] S. Boyd and L. Vandenberghe, *Convex Optimization*, 1st ed. Cambridge Univ. Press, 2004.
- [34] ITU-R Rec. M.1225, *Guidelines for Evaluation of Radio Transmission Technologies for IMT-2000*, ITU-R, Feb. 1997.
- [35] WIGLE.NET: Wireless Geographic Logging Engine, <http://wgle.net/>.
- [36] J. G. Andrews, F. Baccelli, and R. K. Ganti, "A Tractable Approach to Coverage and Rate in Cellular Networks," *IEEE Trans. Commun.*, vol. 59, pp. 3122–3134, Nov. 2011.
- [37] I. S. Gradshteyn, I. M. Ryzhik, and A. Jeffrey, *Table of Integrals, Series, and Products*, 7th ed. Academic Press, 2007.

APPENDIX A DERIVATION OF SINR DISTRIBUTIONS

For the simplicity in presentation, we define a function which represents the impact of the aggregated interference to an MS from multiple interferers, i.e., fBSs, which are randomly located outside the circular region with the radius of D . We assume the pathloss parameters applied to the wireless links between the MS in consideration and interfering fBSs are heterogeneous and given by Z and α . Then, the aggregated interference from the multiple fBSs to the MS is expressed by $I_a = \sum_{i \in \Lambda_D} P_f \Psi_i (Z r_i)^{-\alpha}$, where r_i represents the distance between a specific interferer and the MS, Λ_D represents the set of all the interferers randomly located outside the circular region with the radius D , and Ψ is an independent Rayleigh fading component of link i . Let us assume that the interferers are distributed according to an SPPP distribution with the intensity of λ_I . By generalizing the analysis results in [36], the Laplace transform of I_a , which is defined by $L_{I_a}(s) \triangleq E[e^{-s I_a}]$, is calculated as follows:

$$L_{I_a}(s|P_f, \alpha, Z, \lambda_I, D) = \exp \left(-\pi \lambda_I Z^{-2} (s P_f)^{\frac{2}{\alpha}} \int_{Z^2 D^2 (s P_f)^{-\frac{2}{\alpha}}}^{\infty} \left(\frac{1}{u^{\frac{\alpha}{2}+1}} \right) du \right). \quad (42)$$

From the integral table found in [37], the Laplace transform of I_a is given as follows in the special case that $\alpha = 4$:

$$L_{I_a}(s|P_f, 4, Z, D) = \exp \left(-\pi \lambda_I Z^{-2} \sqrt{s P_f} \left(\frac{\pi}{2} - \tan^{-1} \left(\frac{Z^2 D^2}{\sqrt{s P_f}} \right) \right) \right). \quad (43)$$

Furthermore, in the special case that $D = 0$,

$$L_{I_a}(s|P_f, \alpha, Z, 0) = \exp \left(-\frac{2\pi^2 \lambda_I Z^{-2} (s P_f)^{2/\alpha}}{\alpha \sin(2\pi/\alpha)} \right). \quad (44)$$

A. SINR distribution of an fMS

Although our actual system model does not allow the deployment of an fBS if the distance between the fBS and other fBS is less than $2D_h$, pure SPPP distribution is assumed in the numerical analysis for numerical tractability. Therefore, it is assumed that the interfering fBSs are randomly located according to SPPP with the density of λ_f and the indoor-to-indoor pathloss parameters are applied for the interference links from the other fBSs. If we refer to the interference received by a typical fMS as I_f , the Laplace transform of I_f is given by

$$L_{I_f}(s) = L_{I_a}(s|P_f, \alpha_5, Z_5, 0), \quad (45)$$

where α_5 and Z_5 are the indoor-to-indoor pathloss parameters, and $L_{I_a}(\cdot)$ is given in (44). SINR of a typical fMS is expressed by $\gamma_f = \frac{\Psi(Z_2 r_f)^{-\alpha_2} P_f}{P_N + I_f}$, where r_f is the distance between an fMS and its serving fBS, P_N is the noise power, and Ψ is an independent Rayleigh fading component of the link between an fMS and its serving fBS. Furthermore, Z_2 and α_2 are the indoor pathloss parameters as described in Table 3 of the main manuscript. For the simplicity in presentation, we define $s = \Gamma(Z_2 r_f)^{\alpha_2} P_f^{-1}$. Then, the CCDF of an fMS's SINR is given by

$$\begin{aligned} F_f(\Gamma|r_f) &\triangleq \Pr \left[\frac{\Psi(Z_2 r_f)^{-\alpha_2} P_f}{P_N + I_f} \geq \Gamma \right] \\ &= \Pr[\Psi \geq s(P_N + I_f)] = E_{I_f} [e^{-s(P_N + I_f)}] \\ &= e^{-s P_N} E_{I_f} [e^{-s I_f}] = e^{-s P_N} L_{I_f}(s), \end{aligned} \quad (46)$$

where the third equality holds because Ψ is an exponential random variable, and the last equality comes from the definition of the Laplace transform. From (44), (45), and (46),

$$F_f(\Gamma|r_f) = \exp(-s P_N) \exp \left(-\frac{2\pi^2 \lambda_f Z_5^{-2} (s P_f)^{2/\alpha_5}}{\alpha_5 \sin(2\pi/\alpha_5)} \right). \quad (47)$$

B. SINR distribution of an mMMS

From the constraint that each fBS fully covers its indoor home area, i.e., $d_f \geq D_h$, all the mMMS are located outside building, and outdoor pathloss parameters, i.e., Z_1 and α_1 , are applied for the wireless link between an mMMS and its serving mBS. Because no interference from the fBSs exists, SINR of a typical mMMS is expressed by $\gamma_m = \frac{\Psi(Z_1 r_m)^{-\alpha_1} P_m}{P_N}$, where r_m is the distance between an mMMS and its serving mBS. If we define $s = \Gamma(Z_1 r_m)^{\alpha_1} P_m^{-1}$, the SINR CCDF of an mMMS is obtained by

$$\begin{aligned} F_m(\Gamma|r_m) &= \Pr \left[\frac{\Psi(Z_1 r_m)^{-\alpha_1} P_m}{P_N} \geq \Gamma \right] \\ &= \Pr[\Psi \geq s P_N] = e^{-s P_N}. \end{aligned} \quad (48)$$

C. SINR distribution of an oMS

Let us consider a typical oMS who is located at r_o away from its serving fBS. If we refer to the interference received by the oMS from the other fBSs as I_o , I_o is the sum of interference from the fBSs which are randomly distributed outside the circular region with the radius r_o with the density λ_f . Therefore, the Laplace transform of I_o is given by

$$L_{I_o}(s) = L_{I_a}(s|P_f, \alpha_I, Z_I, \lambda_f, r_o), \quad (49)$$

where Z_I and α_I are the pathloss parameters of the interfering links, and $L_{I_a}(\cdot)$ is given in (42). If we refer to the pathloss parameters of the desired link to the serving fBS as Z_d and α_d , the SINR of a typical fMS is expressed by $\gamma_o = \frac{\Psi(Z_d r_o)^{-\alpha_d} P_f}{P_N + I_o}$. Similarly to (46), the CCDF of an oMS's SINR is

$$F_o(\Gamma|r_o) = e^{-sP_N} L_{I_a}(s|P_f, \alpha_I, Z_I, \lambda_f, r_o), \quad (50)$$

where $s = \Gamma(Z_d r_o)^{\alpha_d} P_f^{-1}$. From the system model, $(Z_d, \alpha_d, Z_I, \alpha_I) = (Z_4, \alpha_4, Z_4, \alpha_4)$ if the oMS is an outdoor user, i.e., $r_o \geq D_h$. On the other hand, $(Z_d, \alpha_d, Z_I, \alpha_I) = (Z_2, \alpha_2, Z_5, \alpha_5)$ if $r_o < D_h$. In our system model, $\alpha_I = 4$ because $\alpha_4 = \alpha_5 = 4$. Therefore, $L_{I_a}(\cdot)$ in (43) is utilized to obtain the SINR CCDF of an oMS, and hence

$$F_o(\Gamma|r_o) = \exp\left(-\frac{\pi\lambda_f\sqrt{sP_f}}{Z_I^2}\left(\frac{\pi}{2} - \tan^{-1}\left(\frac{Z_I^2 r_o^2}{\sqrt{sP_f}}\right)\right) - sP_N\right), \quad (51)$$

where

$$(Z_I, s) = \begin{cases} (Z_4, P_f^{-1}\Gamma(Z_4 r_o)^{\alpha_4}), & r_o \geq D_h, \\ (Z_5, P_f^{-1}\Gamma(Z_2 r_o)^{\alpha_2}), & \text{otherwise.} \end{cases} \quad (52)$$

APPENDIX B PROOFS OF PROPOSITIONS

A. Proof of Proposition 1

If x is given by a fixed value and the value is feasible, the optimization problem becomes a linear programming (LP) problem with a single variable ρ . By rephrasing the constraint (35) of the main manuscript, we obtain that $0 \leq \frac{t_m(x)}{t_{fo}(x) + t_m(x)} \leq \rho \leq 1$. Because $t_m(x) > 0$, the objective is maximized when ρ is the minimum value. By the definition of x^* , the objective is maximized when $(\rho, x) = \left(\frac{t_m(x^*)}{t_{fo}(x^*) + t_m(x^*)}, x^*\right)$.

B. Proof of Proposition 2

In the fMS's benefit requirement limited environments, t_{fo} and t_m are respectively given by

$$t_{fo}(x) = \frac{\bar{B}_f(1 - e^{-\lambda_u x})}{M\lambda_u x} \quad (53)$$

$$t_m(x) = \frac{\bar{B}_m(1 - e^{-A_m\lambda_u(1-\lambda_f)x})}{A_m\lambda_u(1-\lambda_f x)}. \quad (54)$$

From Proposition 1, we can replace ρ in the formulated problem in (34) of the main manuscript with $\frac{t_m(x)}{t_{fo}(x) + t_m(x)}$

Then, the objective function becomes a single-variable function, i.e., $\frac{t_m(x)t_{fo}(x)}{t_{fo}(x) + t_m(x)}$. Accordingly, the optimization problem is equivalent to the following single-variable minimization problem:

$$\min_x \frac{M\lambda_u x}{\bar{B}_f(1 - e^{-\lambda_u x})} + \frac{A_m\lambda_u(1 - \lambda_f x)}{\bar{B}_m(1 - e^{-A_m\lambda_u(1-\lambda_f)x})} \quad (55)$$

s.t.

$$\frac{1 - e^{-\pi D_h^2 \lambda_f}}{\lambda_f} \leq x \leq \frac{1 - e^{-\pi D_{\max}^2 \lambda_f}}{\lambda_f}, \quad (56)$$

where the objective function is a reciprocal of the objective in the original problem.

It is well known that the minimization problem which has only the linear constraints is a convex problem if the objective function is convex [33]. We prove that (55) is a convex function by showing that both the first and second terms of (55) are convex.

First, we show that the second derivative of the first term of (55) is always positive when $x > 0$. The second derivative of $\frac{\lambda_u x}{\bar{B}_f(1 - e^{-\lambda_u x})}$ is calculated by

$$\lambda_u^2 \bar{B}_f^{-1} e^{-y} (1 - e^{-y})^{-3} [(y+2)e^{-y} + y - 2], \quad (57)$$

where $y \triangleq \lambda_u x > 0$. Because $\lambda_u^2 \bar{B}_f^{-1} e^{-y} (1 - e^{-y})^{-3} \geq 0$ when $y > 0$, the first term of (55) is convex if $[(y+2)e^{-y} + y - 2] \geq 0$ when $y > 0$. Clearly, the above inequality holds when $y \geq 2$, because both $(y+2)e^{-y}$ and $y - 2$ are positive when $y \geq 2$. When $0 < y < 2$, we need to prove that $e^{-y} \geq \frac{2-y}{2+y}$, and it is satisfied if $\frac{d}{dy}[e^{-y}] \geq \frac{d}{dy}\left[\frac{2-y}{2+y}\right]$ because $[e^{-y}]_{y=0} = \left[\frac{2-y}{2+y}\right]_{y=0}$. It is equivalent to prove that $e^y \geq \frac{(y+2)^2}{4}$ in the region. We complete the proof by showing that the following three inequalities hold: $[e^y]_{y=0} \geq \left[\frac{(y+2)^2}{4}\right]_{y=0}$, $\frac{d}{dy}[e^y]_{y=0} \geq \frac{d}{dy}\left[\frac{(y+2)^2}{4}\right]_{y=0}$, and $\frac{d^2}{dy^2}[e^y]_{y \geq 0} \geq \frac{d^2}{dy^2}\left[\frac{(y+2)^2}{4}\right]_{y \geq 0}$, where the detailed calculations are omitted.

Second, we prove that the second term of (55) is also convex. We define a new parameter $z = A_m(1 - \lambda_f x)$. Then, the second term of (55) can be expressed by $\frac{\lambda_u z}{\bar{B}_m(1 - e^{-\lambda_u z})}$, which is the same form as the first term of (55). According to the above derivations in this appendix, $\frac{\lambda_u z}{\bar{B}_m(1 - e^{-\lambda_u z})}$ is a convex function of z . Because an affine mapping preserves the convexity [33], the second term of (55) is also a convex function of x .

C. Proof of Proposition 3

If we define $C(x) \triangleq \frac{(1 - e^{-\lambda_u x})}{\lambda_u x}$ and $D(x) \triangleq \frac{(\lambda_u x + e^{-\lambda_u x} - 1)}{(\lambda_u x)^2}$, the average throughputs of an fMS and an oMS are respectively given by $\bar{T}_f(\rho, x) = \rho W \bar{B}_f C(x)$ and $\bar{T}_o(\rho, x) = \rho W \bar{B}_o D(x)$. Then, the condition that a given environment is the fMS's requirement-limited environment is expressed by $\frac{\bar{B}_f C(x)}{\bar{B}_o D(x)} \leq \frac{M}{K}$ for all $x \in [X_{\min}, X_{\max}]$. If the

conditions $\frac{d}{dx} [\bar{B}_o(x)] \leq 0$ and $\frac{d}{dx} \left[\frac{D(x)}{C(x)} \right] \geq 0$ are satisfied in the all feasible x , $\frac{\bar{B}_f C(X_{\min})}{\bar{B}_o(X_{\max}) D(X_{\min})} \leq \frac{M}{K}$ is a sufficient condition that a given environment is the fMS's requirement-limited environment because

$$\frac{\bar{B}_f C(x)}{\bar{B}_o(x) D(x)} \leq \frac{\bar{B}_f}{\bar{B}_o(X_{\max}) C^{-1}(X_{\min}) D(X_{\min})} \leq \frac{M}{K}. \quad (58)$$

Therefore, we complete the proof by showing that $\frac{d}{dx} [\bar{B}_o(x)] \leq 0$ and $\frac{d}{dx} \left[\frac{D(x)}{C(x)} \right] \geq 0$. Firstly, it is trivial that $\frac{d}{dx} [\bar{B}_o(x)] \leq 0$ because the average transmission rate of oMSs should be decreased by expanding the service radius of the femtocells. Secondly, we show that $\frac{d}{dy} \left[\frac{D(y/\lambda_u)}{C(y/\lambda_u)} \right] \geq 0$ which is equivalent to $\frac{d}{dx} \left[\frac{D(x)}{C(x)} \right] \geq 0$, where $y = \lambda_u x$. We need to show that $\frac{d}{dy} \left[\frac{e^{-y} + y - 1}{y(1 - e^{-y})} \right] \geq 0$ in the whole feasible region of y , and the condition is equivalent to

$$\frac{5}{4} \geq \left(e^{-y} - \frac{1}{2} \right)^2 + e^{-y} (y - 1)^2, \quad (59)$$

and the above inequality holds if both $\frac{1}{4} \geq (e^{-y} - \frac{1}{2})^2$ and $e^y \geq (y - 1)^2$ are satisfied in $y \geq 0$. It is trivial that $\frac{1}{4} \geq (e^{-t} - \frac{1}{2})^2$ because $0 \leq e^{-y} \leq 1$ when $y \geq 0$. Furthermore, $e^y \geq (y - 1)^2$ when $0 \leq y \leq 1$ because $e^y \geq 1$ and $\frac{d}{dy} (y - 1)^2 < 0$ in the region. When $y \geq 1$, it can be shown that $e^y \geq (y - 1)^2$ because the following three inequalities hold: $[e^y]_{y=1} \geq [(y - 1)^2]_{y=1}$, $\frac{d}{dy} [e^y]_{y=1} \geq \frac{d}{dy} [(y - 1)^2]_{y=1}$, and $\frac{d^2}{dy^2} [e^y]_{y=1} \geq \frac{d^2}{dy^2} [(y - 1)^2]_{y=1}$.

D. Proof of Proposition 4

We define $f(t) \triangleq \frac{t}{1 - e^{-t}}$ and its first derivative as $f'(t)$. Then, the first derivatives of the first and second terms of (55) are given by $\frac{M\lambda_u}{B_f} f'(t)|_{t=\lambda_u x}$ and $-\frac{\lambda_u \lambda_f A_m}{B_m} f'(t)|_{t=A_m \lambda_u (1 - \lambda_f x)}$, respectively. Hence, if $\frac{\lambda_f A_m}{B_m} = \frac{N_f}{B_m} > \frac{M}{B_f}$ and $f'(A_m \lambda_u (1 - \lambda_f x)) \geq f'(\lambda_u x)$ always hold in the feasible region of x , the maximum cell coverage is optimal. According to the derivation in Appendix A, $f'(t)$ is an increasing function of t . Accordingly, $f'(A_m \lambda_u (1 - \lambda_f x)) \geq f'(\lambda_u x)$ always holds if $A_m \lambda_u (1 - \lambda_f x (D_{\max})) \geq \lambda_u x (D_{\max})$. The last condition represents that the average number of users in a macrocell is larger than the average number of users in a single femtocell with the maximum cell coverage, and the condition is satisfied in the general environments. Therefore, $\frac{N_f \bar{B}_f}{M \bar{B}_m} > 1$ is a sufficient condition that the optimal femtocell coverage is the maximum value in the general environments.

E. Proof of Proposition 5

The objective function of our load balancing scheme is not a function of β . Instead, β only influences the feasible

region of the other control parameters (ρ, x) determined by the constraints. From (4) and (5) of the main manuscript, the constraint related to β is given by

$$\min \left(\frac{\bar{T}_f(\rho, x, \beta)}{M}, \frac{\bar{T}_o(\rho, x, \beta)}{K} \right) \geq \bar{T}_m(\rho, x). \quad (60)$$

Because the right side of the above inequality is the objective function of our optimization problem, β which maximizes the left side of the above inequality is an (or one of) optimal parameter(s) which maximizes the objective function of the original problem, i.e.,

$$\beta^*(\rho, x) = \arg \max_{\beta} \min \left(\frac{\bar{T}_f(\rho, x, \beta)}{M}, \frac{\bar{T}_o(\rho, x, \beta)}{K} \right), \quad (61)$$

s.t. $0 \leq \beta \leq 1$.

At a given (ρ, x) , we refer to the solution of β which solves the equation $\frac{\bar{T}_f(\rho, x, \beta)}{M} = \frac{\bar{T}_o(\rho, x, \beta)}{K}$ as Q . It is easy to show that $\bar{T}_f(\rho, x, \beta)$ and $\bar{T}_o(\rho, x, \beta)$ are monotonically increasing and decreasing functions of β , respectively. Due to the monotonicity of the two functions, the solution real value Q always exists, and $\min \left(\frac{\bar{T}_f(\rho, x, \beta)}{M}, \frac{\bar{T}_o(\rho, x, \beta)}{K} \right)$ is an increasing function when $\beta < Q$ and a decreasing function when $\beta \geq Q$. Therefore, the optimal parameter β^* maximizing (61) in the range of $\beta \in [0, 1]$ is given by

$$\beta^* = \begin{cases} Q, & 0 \leq Q \leq 1, \\ 0, & Q < 0, \\ 1, & Q > 1. \end{cases} \quad (62)$$

From the definition of $A(x)$, $B(x)$, $C(x)$, and $D(x)$ in Proposition 5, $\frac{\bar{T}_f(\rho, x, \beta)}{M} = W\rho\beta(B(x) - C(x)) + W\rho C(x)$ and $\frac{\bar{T}_o(\rho, x, \beta)}{K} = W\rho(1 - \beta)D(x)$. Accordingly, Q is calculated by

$$Q = \frac{D(x) - C(x)}{B(x) + D(x) - C(x)}. \quad (63)$$

Because $B(x)$, $C(x)$, and $D(x)$ are positive in the region of interest, $Q \leq 1$. From (62) and (63), we obtain the optimal β^* as a function of x as follows:

$$\beta^*(x) = \begin{cases} \frac{-C(x) + D(x)}{B(x) - C(x) + D(x)}, & D(x) \geq C(x) \\ 0, & \text{otherwise,} \end{cases} \quad (64)$$

By using β^* , the load balancing problem in hybrid access femtocell networks can be rephrased by inserting

$$t_{fo}(x) = \begin{cases} \frac{B(x)D(x)}{B(x) + D(x) - C(x)}, & D(x) \geq C(x), \\ D(x), & \text{otherwise,} \end{cases} \quad (65)$$

into (35) of the main manuscript. Because Proposition 1 still holds,

$$\rho^*(x) = \begin{cases} \frac{\frac{A(x)}{B(x) - C(x) + D(x)}}{\frac{A(x)}{D(x) + A(x)}}, & D(x) \geq C(x), \\ \frac{A(x)}{D(x) + A(x)}, & \text{otherwise.} \end{cases} \quad (66)$$

APPENDIX C

DISCUSSION FOR ORTHOGONAL DEPLOYMENT AND ITS APPLICATIONS

Generally, co-channel deployment of femtocells might be preferred because the spectral efficiency can be maximized by the co-channel deployment. However, we in this paper propose a load balancing scheme in two-tier cellular networks based on the orthogonal channel deployment, and the evaluation results have shown that the orthogonal channel deployment can be beneficial in some aspects. The advantages of the orthogonal channel deployment inferred by this paper are summarized as follows:

- 1) Orthogonal deployment can enhance the maximum service coverage of femtocells by removing the cross-tier interference from macrocells, and it is beneficial to increase the amount of macrocell load transferred to femtocells. Many macrocell users can be served by open and hybrid access femtocells in the orthogonal deployment.
- 2) The service quality provided to each type of users can be flexibly controlled. Therefore, the mobile operators can adaptively select the system parameters to provide the ‘adequate’ service quality for each type of users based on its own policy. The ‘adequate’ service quality can be very different according to the deployment

environment, market status, and characteristics of end consumers.

Considering orthogonal deployment’s capability for no cross-tier interference and the large coverage provisioning, orthogonal deployment can be beneficial in the following conditions:

- 1) The traffic load in the macrocell is so high that large traffic offloading from macrocell area is essential, and/or
- 2) Service area is not perfectly covered by macrocell area so that the femtocells are expected to help the service coverage extension, and/or
- 3) The fMSs do not require the large performance benefit from using femtocells so that it is not necessary to allocate the whole resources to fMSs and oMSs as co-channel deployment based schemes do, and/or
- 4) The end consumers are not willing to spend much money to use the femtocell service so that the financial benefits obtained by solely femtocell selling is not expected to be very large, and/or
- 5) The cost reduction due to the reduced macrocell deployment or increased benefit obtained from the enhanced macrocell user performance is expected to be significant.